

Protecting logical qubits with dynamical decoupling

Jia-Xiu Han,^{1,2,*} Jiang Zhang,^{1,*} Guang-Ming Xue,^{1,2} Haifeng Yu,^{1,2,†} and Guilu Long^{1,3,4,5,‡}

¹*Beijing Academy of Quantum Information Sciences, Beijing 100193, China*

²*Hefei National Laboratory, Hefei 230088, China*

³*State Key Laboratory of Low-Dimensional Quantum Physics and
Department of Physics, Tsinghua University, Beijing 100084, China*

⁴*Frontier Science Center for Quantum Information, Beijing 100084, China*

⁵*Beijing National Research Center for Information Science and Technology, Beijing 100084, China*

Demonstrating that logical qubits outperform their physical counterparts is a milestone for achieving reliable quantum computation. Here, we propose to protect logical qubits with a novel dynamical decoupling scheme that implements iSWAP gates on nearest-neighbor physical qubits, and experimentally demonstrate the scheme on superconducting transmon qubits. In our scheme, each logical qubit only requires two physical qubits. A universal set of quantum gates on the logical qubits can be achieved such that each logical gate comprises only one or two physical gates. Our experiments reveal that the coherence time of a logical qubit is extended by up to 366% when compared to the better-performing physical qubit. Moreover, to the best of our knowledge, we demonstrate for the first time that multiple logical qubits outperform their physical counterparts in superconducting qubits. We illustrate a set of universal gates through a logical Ramsey experiment and the creation of a logical Bell state. Given its scalable nature, our scheme holds promise as a component for future reliable quantum computation.

Introduction.—Physical qubits are fundamental building blocks of quantum computers but are inherently susceptible to errors due to unavoidable interactions with their environment [1, 2]. To perform reliable quantum computation, one needs to employ logical qubits which are defined using a set of physical qubits [3]. It is a milestone to demonstrate that logical qubits outperform their associated physical counterparts, known as the “break-even point” [4–7]. One available approach to achieving this goal is to utilize quantum error correction (QEC) [3, 8–15]. Despite impressive achievements, connecting multiple logical qubits presents a significant challenge for these schemes. To perform quantum algorithms with logical qubits before large-scale QEC are realized, it is still intriguing to investigate scalable error-mitigation or error-suppressing schemes for protecting logical qubits.

Dynamical decoupling (DD) (for reviews, see [3, 16]) can manipulate interactions between a set of physical qubits and their environment by applying tailored control pulses to the qubits. One method is to completely eliminate these interactions, isolating the evolution of qubits [17–28]. Another method is to selectively eliminate non-collective interactions while preserving collective ones, in which the qubits interact with the environment in a uniform manner [29–32]. The latter introduces decoherence-free subspaces (DFS) and noiseless subsystems (NS), allowing logical qubits to be encoded, immune to collective errors. Previous pioneering work has demonstrated how to optimally generate collective interactions using DD sequences consisting of SWAP gates [32]. In this scenario, all types of collective interactions are kept by SWAP operations, and thus rather complex encoding and decoding procedures are required to store and retrieve information with logical qubits. Logical operations on these logical qubits generally demand multi-body interactions,

which are complicated to realize in practical. Moreover, SWAP gates cannot be directly implemented on various quantum computing platforms. As a result, an ideal DD scheme for protecting logical qubits is expected to utilize directly realizable quantum gates and generate DFSs in which logical qubits can be defined with simple encoding and decoding procedure as well as experimentally feasible logical gates.

In this work, we propose to generate Z -type collective interactions for physical qubits by periodically performing iSWAP gates. While the Z -type collective interactions are created, the X - and Y -type interactions are removed from the system evolution. Compared with existing DD works in superconducting qubits [33–37], our scheme can be regarded as many-body DD [38]. The resulting Z -type collective interaction supports a DFS, enabling the encoding of logical qubits, each of which requires only two physical qubits. One feature of our scheme is scalability, and generating collective interactions for multiple qubits requires only iSWAP gates between nearest-neighbor qubits. Furthermore, universal gates for logical qubits can be realized using single-body and nearest-neighbor two-body Hamiltonians. We experimentally demonstrate that the coherence time of a protected logical qubit is extended by up to 366% compared to that of the better-performing physical qubit. For two logical qubits, the process fidelity is 194% compared to that of the physical qubits at a duration of $\tau = 4.8 \mu\text{s}$. To the best of our knowledge, this is the first time that multiple logical qubits have been shown to outperform their physical counterparts in superconducting qubits. To showcase the universal control of logical qubits, we conduct a logical Ramsey experiment on one of the logical qubits and create a logical Bell state with logical operations. Additionally, we demonstrate that our scheme

can enhance the success probability in superdense coding as an application.

Protecting logical qubits with iSWAP gates.—We begin by explaining how to encode a single logical qubit using a pair of physical qubits. When two qubits interact with their environment, the interaction Hamiltonian can be written as

$$H_I = \sum_{\alpha=x,y,z} \sigma_{\alpha}^1 \otimes E_{\alpha}^1 + \sigma_{\alpha}^2 \otimes E_{\alpha}^2, \quad (1)$$

where σ_{α}^k represents the Pauli- α operator acting on the k th qubit, and E_{α}^k is the related environmental Hamiltonian [18]. H_I may cause dephasing and dissipation to the qubits, distorting the evolution of the physical qubits. The independent interaction H_I can be transformed into a collective one using the DD procedure D_2 (shown in Fig. 2(c)) which consists of four iSWAP gates applied in equal time interval. The obtained effective Hamiltonian $H_I^z = S_z \otimes \bar{E}_z$, with $S_z = (\sigma_z^1 + \sigma_z^2)/2$ and $\bar{E}_z = E_z^1 + E_z^2$, is a Z -type collective interaction [39].

H_I^z supports a DFS, denoted as $\text{DFS}_2 = \text{Span}\{|01\rangle, |10\rangle\}$, which serves as the encoding space for a logical qubit defined as $|0\rangle_L = |01\rangle$ and $|1\rangle_L = |10\rangle$. Since the two logical bases vanish under the action of H_I^z , they are dark states of H_I^z and thus unaffected by it. The encoding and decoding procedures of the logical qubits are explicitly shown in Fig. 2(a) and (b). Due to the fact that the encoding and decoding procedures of DFS_2 are concise, it is also used in other schemes, such as g -frame qubit [38], hardware-efficient architecture [40], and dual-rail qubits [41–44]. Two logical qubits can be encoded with four physical qubits in a four-dimensional DFS, denoted as $\text{DFS}_4 = \text{Span}\{|00\rangle_L, |01\rangle_L, |10\rangle_L, |11\rangle_L\}$. The DFS_4 is supported by a four-qubit Z -type collective interaction which can be generated with the procedure D_4 illustrated in Fig. 2(c). Our protective scheme is scalable in the sense that for N logical qubits, we can also implement a DD procedure to generate a $2N$ -qubit Z -type collective interaction which supports a 2^N -dimensional DFS [39].

Experimental demonstration of protecting logical qubits.—In our experiments, we utilize a superconducting device consisting of four frequency-tunable transmon qubits. Fig. 1 shows the configuration of the device: the four physical qubits Q_1 to Q_4 are arranged in a circle with only nearest-neighbor coupling, and adjacent qubits are connected through tunable couplers [45], labeled as C_{12} to C_{14} . Each qubit connects to a dedicated driving line for individual XY control. The coupling strength between neighboring qubits can be adjusted from negative to positive by tuning the couplers' resonance frequencies. This adjustability ensures the high-contrast on-off switching of inter-qubit coupling, which is essential for implementing entangling gates such as iSWAP and controlled-Z (CZ) gates [46]. Additionally, we employ impedance-matched Josephson parameter amplifiers

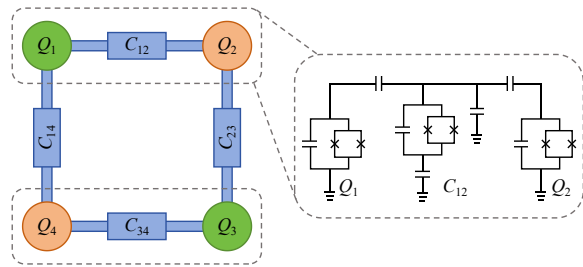


FIG. 1. Arrangement of physical and logical qubits. Left: the physical qubits are denoted by green and orange circles. Interactions (C_{12} to C_{14}) between physical qubits are labeled with blue rectangles. Physical qubits Q_1 and Q_2 are used to define the logical qubit L_1 , while Q_3 and Q_4 constitute the logical qubit L_2 . Right: the schematic circuit of the device including two transmon qubits and one tunable coupler.

(JPAs) to achieve high-fidelity single-shot readout of the qubits [47].

We assess the memory times of both logical and physical qubits by employing quantum process tomography [1] to quantify the fidelities of identity operation across various durations (for details, see [39]). We begin by evaluating the performance of the logical qubit L_1 and its physical counterparts. From Fig. 2(d), one can see that without any protection mechanisms, the process fidelities of physical qubits Q_1 and Q_2 noticeably decrease with increasing duration τ . The fidelity for the physical qubit Q_i can be written as [39, 48, 49]

$$F_{Q_i} = \frac{1}{4} \left(2e^{-(\tau/T_{2,i})^2} + e^{-\tau/T_{1,i}} + 1 \right), \quad (2)$$

where $T_{2,i}$ and $T_{1,i}$ represent the coherence and energy relaxation times of physical qubit Q_i , respectively.

Without protection, L_1 experiences a more rapid fidelity degradation than a single physical qubit since two physical qubits introduce more errors, with the unprotected logical coherence time $T_2^{\text{un}} = T_{2,1}T_{2,2}/(T_{2,1} + T_{2,2})$ and the energy relaxation time $T_{1,1}$. The fidelity of unprotected L_1 is affected by T_1 error only from Q_1 due to the tailored decoding procedure [39].

Remarkably, when L_1 is protected by D_2 , the process fidelity of L_1 decreases much more slowly than that of unprotected L_1 as well as that of any physical qubits. For instance, at $\tau = 6.0 \mu\text{s}$, the process fidelity of L_1 remains 72.31%, significantly higher than the 49.59% observed for the better-performing physical qubit Q_1 . Compared with the Gaussian decay observed in the fidelity of physical qubits, the protected L_1 exhibits an exponential decay in process fidelity

$$F_{L_1} = \frac{1}{4} \left(2e^{-\tau/T_2^{\text{P}}} + e^{-\tau/T_{1,1}} + 1 \right), \quad (3)$$

since the environment around L_1 is modified by D_2 . A prolonged logical coherence time $T_2^{\text{P}} = 9.2 \mu\text{s}$ is found

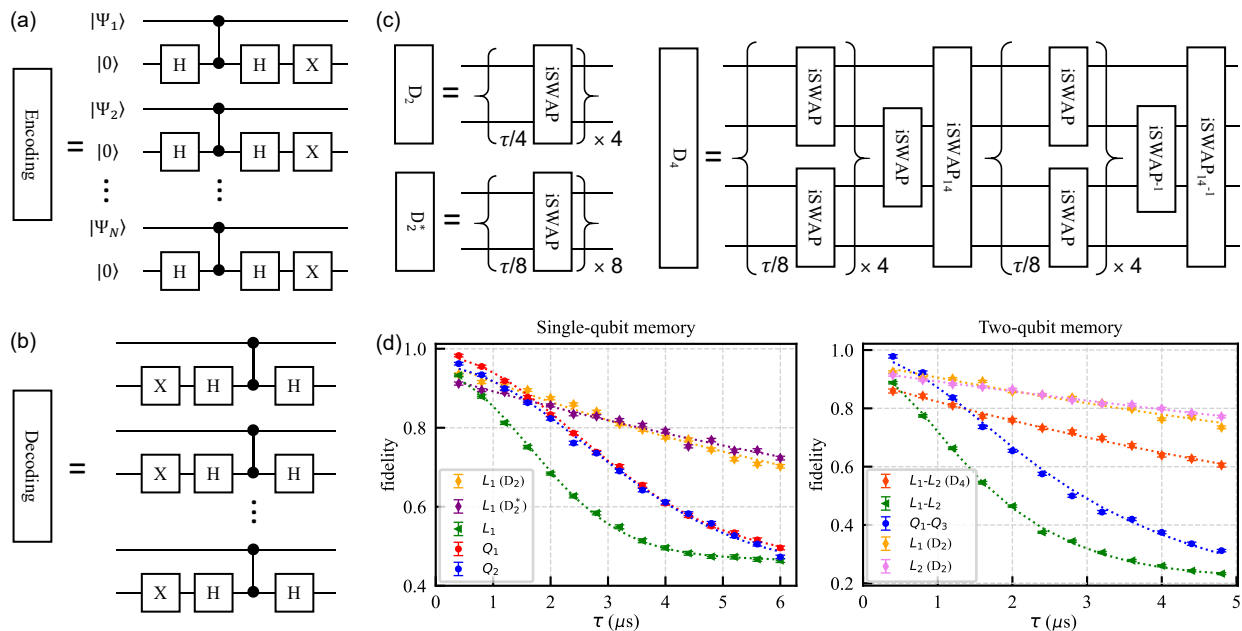


FIG. 2. Quantum circuits and process fidelities for various procedures. (a) Encoding circuit for N -logical qubits. (b) Decoding circuit for N -logical qubits. (c) Quantum circuits of D_2 , D_2^* , and D_4 . (d) Left: Process fidelities of single-qubit identity operation over increased durations. Right: Process fidelities of two-qubit identity operation over increased durations. Details are shown in the inset. Dashed lines are fitting curves plotted using the fidelity functions [39].

from F_{L_1} , far exceeding the coherence times of physical qubits $T_{2,1} = 3.8 \mu\text{s}$ and $T_{2,2} = 4.2 \mu\text{s}$.

We also implement a procedure D_2^* which uses eight iSWAPs to protect L_1 , shown in Fig. 2(c). The application of D_2^* increases the logical coherence time to $T_2^* = 12.5 \mu\text{s}$. Hence, our results convincingly verify that the memory of the protected logical qubit surpasses that of the better-performing physical qubit. We expect that longer logical coherence time can be obtained with more iSWAP gates applied in a protecting procedure.

We further evaluate the performance of two logical qubits protected by D_4 shown in Fig. 2(c). To achieve precise quantum operations, we reconfigure the operating frequencies of the four physical qubits and recalibrate the associated gates. Illustrated in Fig. 2(d), we replicate the single-logical-qubit experiments with procedure D_2 on both L_1 and L_2 , resulting in a maximum 366% increase in the coherence time of logical qubit L_2 ($15.0 \mu\text{s}$), compared to the coherence time of the better-performing physical qubit Q_4 ($4.1 \mu\text{s}$). Moreover, the two-logical-qubit process, protected by D_4 , exhibits significant improvement over the two-physical-qubit process, as shown in Fig. 2(d). When $\tau = 4.8 \mu\text{s}$, the fidelity of the former remains 60.51%, significantly surpassing that of the latter (31.19%).

In our experiments, we observe a trade-off between mitigating environmental errors and introducing control errors through the protection procedure. Here, we chose to employ unoptimized quantum gates, because we are more concerned about the declining trend of process fi-

delity. It is reasonable to anticipate that utilizing quantum gates with higher fidelity could shift the onset of this trade-off to an earlier time, potentially enhancing the fidelity of logical qubits.

Universal operations for logical qubits.—Our scheme enables universal control of logical qubits using single-body and nearest-neighbor two-body Hamiltonians (see Fig. 3(a)). The logical Pauli- z operator for L_1 ($\sigma_z^{L_1}$) is just the physical σ_z^1 operator. Then, for logical qubit L_1 , a logical rotation R_z^φ about the z -axis by an angle φ is equivalent to the same rotation of physical qubit Q_1 . The logical Pauli- x operator for L_1 ($\sigma_x^{L_1}$) is represented by the XY-interaction $\sigma_x^1 \sigma_x^2 + \sigma_y^1 \sigma_y^2$. It follows that the $\sqrt{\text{iSWAP}}$ gate acting on Q_1 and Q_2 is the logical rotation $R_x^{-\pi/2}$ about the x -axis by an angle $-\pi/2$ for L_1 . With these two logical rotations available, we can perform an arbitrary operation, such as the logical Hadamard gate (H), on a logical qubit. Additionally, the $\sigma_z^{L_1} \sigma_z^{L_2}$ interaction between L_1 and L_2 corresponds to the physical $\sigma_z^2 \sigma_z^3$, which is a nearest-neighbor interaction between Q_2 and Q_3 . Hence, a logical CZ gate can be achieved by implementing a CZ gate between Q_2 and Q_3 followed by a R_z^π gate on Q_3 . As a result, we can establish a complete set of universal logical gates: $\{R_z^\varphi, R_x^{-\pi/2}, \text{CZ}\}$.

To demonstrate single-qubit logical operations, we conduct a logical Ramsey experiment on L_1 , incorporating the logical operations depicted in Fig. 3(b). The experimental data closely aligns with the simulation results, which are calculated based on the energy relaxation time

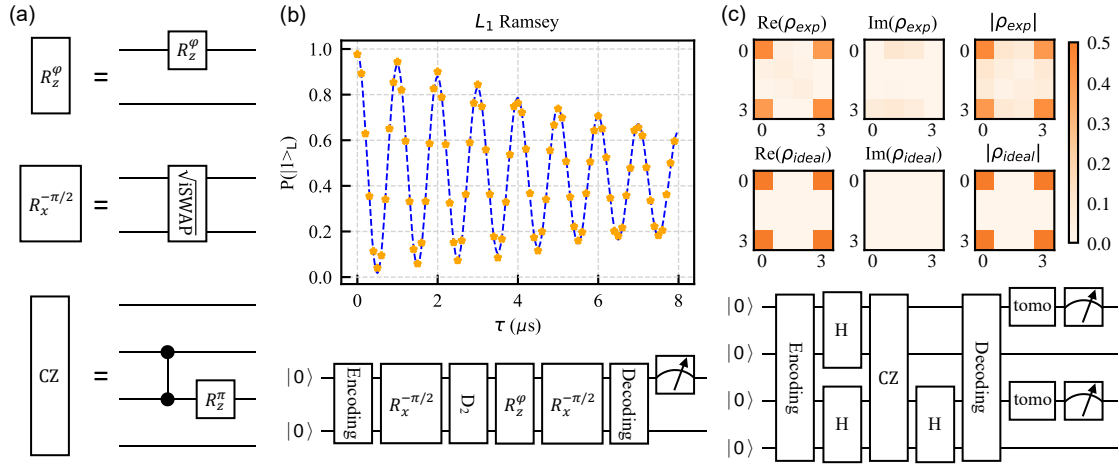


FIG. 3. Universal logical operations. (a) The set of universal logical gates. (b) A Ramsey experiment is conducted on logical qubit L_1 . The orange stars represent experimental data points, while the blue dashed line indicates the simulation results. (c) Preparation of the logical Bell state $B_1 = (|00\rangle_L + |11\rangle_L)/\sqrt{2}$ from initial state $|00\rangle_L$ using logical Hadamard and CZ gates. The obtained density matrix elements are shown in the top, where 0 to 3 represent the bases $|00\rangle$, $|01\rangle$, $|10\rangle$, and $|11\rangle$, respectively.

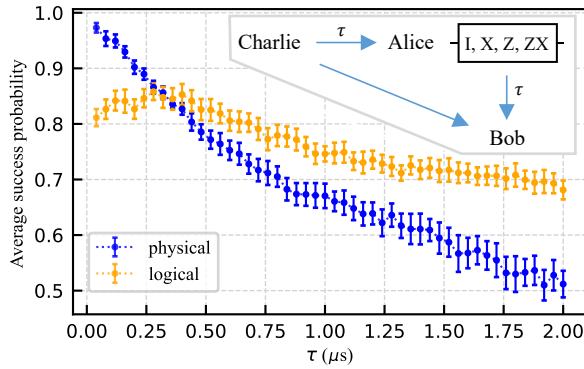


FIG. 4. Superdense coding. The average success probabilities for logical superdense coding (illustrated in orange) and physical superdense coding (illustrated in blue).

$T_{1,1}$ and the coherence time T_2^p as input parameters.

The universal logical control is finally illustrated by preparing a logical Bell state $B_1 = (|00\rangle_L + |11\rangle_L)/\sqrt{2}$ on L_1 and L_2 , shown in Fig. 3(c). We utilize quantum state tomography to evaluate the state's fidelity, which is determined to be 92.30%. Our analysis indicates that about 28% of the errors originate from the state tomography and readout process. The remaining errors predominantly arise from operations involving physical two-qubit gates ($\sqrt{\text{ISWAP}}$ and CZ). We stress that the main focus here is to show that universal control is available in our scheme. Hence, we choose a rather tedious circuit which comprises 7 layers and 11 two-qubit gates to create B_1 . In practice, a more concise method is to prepare a Bell state for two physical qubits and then apply the encoding procedure. The latter method uses much fewer two-qubit gates and thus will obtain a higher state fidelity for B_1 .

Application to superdense coding.—As an application, we demonstrate the utility of logical qubits in enhancing the performance of superdense coding [50]. The process is illustrated in the inset of Fig. 4.

Initially, a trusted third party Charlie prepares the Bell state B_1 . Then, Charlie sends one qubit to Alice and the other to Bob, assuming that this transmission takes time τ . Upon receiving her qubit, Alice applies one of the four possible operations ($\{I, X, Z, ZX\}$) to it and then forwards it to Bob, which process takes the other τ . Bob then performs a Bell measurement, yielding four possible outcomes according to Alice's operations. This allows Bob to extract the information transmitted by Alice after a total duration of 2τ . We vary the duration τ to observe its impact on Bob's average success probability.

The experiments are conducted with both physical and logical qubits. For short τ , the physical qubits outperform the logical ones because more control errors are introduced to the logical qubits. However, in a relatively long τ , the logical qubits surpass the physical ones.

Discussion and Conclusion.—Before proceeding further, we would like to provide some remarks on the differences between our scheme and existing works. First, widely used single-body DD schemes, such as XY- N ($N = 4, 8$ and others) sequences, are unsuitable for protecting logical qubits since they can flip the logical states out of the DFS. However, combining the well-developed high-order DD [25] and optimal control [51] with our scheme may enhance its performance. Secondly, the code in our scheme shares similarities with some recent works [40–44]. The key feature of our scheme is that quantum states can be transferred from a logical qubit to one of its physical counterparts and vice versa, making our scheme compatible with other logical qubit protection schemes,

such as QEC.

Our scheme can protect logical qubits from T_2 errors, but cannot eliminate T_1 errors. In the next step, we may use the second physical qubit in a logical qubit as a herald qubit and apply feedback control to compensate it. Then, one may consider developing dynamically protected logical gates for the logical qubits to perform practical quantum algorithms.

In conclusion, we have proposed and verified protection of logical qubits using DD. We have explicitly demonstrated that the lifetimes of both single- and two-logical qubits are prolonged compared to those of their physical counterparts. Also, we conducted a logical Ramsey experiment and successfully created a logical Bell state to illustrate the universal control of the logical qubits. Furthermore, we have shown that our scheme can enhance the success probability in superdense coding.

We acknowledge fruitful discussions with Feihao Zhang. J.H. acknowledges support by the National Natural Science Foundation of China (No. 12004042). J.Z. acknowledges support by the National Natural Science Foundation of China (No. 12004206). H.Y. acknowledges support by the Innovation Program for Quantum Science and Technology (No. 2021ZD0301800) and National Natural Science Foundation of China (No. 92365206). G.L. acknowledges support by the National Natural Science Foundation of China (No. 62131002), Beijing Advanced Innovation Center for Future Chip (ICFC), and Tsinghua University Initiative Scientific Research Program.

* These authors contributed equally to this work.

† hfyu@baqis.ac.cn

‡ gllong@mail.tsinghua.edu.cn

- [1] M. A. Nielsen and I. L. Chuang, Quantum computation and quantum information (Cambridge university press, 2010).
- [2] P. Krantz, M. Kjaergaard, F. Yan, T. P. Orlando, S. Gustavsson, and W. D. Oliver, *Appl. Phys. Rev.* **6**, 021308 (2019).
- [3] D. A. Lidar and T. A. Brun, Quantum error correction (Cambridge university press, 2013).
- [4] M. H. Devoret and R. J. Schoelkopf, *Science* **339**, 1169 (2013).
- [5] N. Ofek, A. Petrenko, R. Heeres, P. Reinhold, Z. Leghtas, B. Vlastakis, Y. Liu, L. Frunzio, S. Girvin, L. Jiang, et al., *Nature* **536**, 441 (2016).
- [6] V. Sivak, A. Eickbusch, B. Royer, S. Singh, I. Tsioutsios, S. Ganjam, A. Miano, B. Brock, A. Ding, L. Frunzio, et al., *Nature* **616**, 50 (2023).
- [7] Z. Ni, S. Li, X. Deng, Y. Cai, L. Zhang, W. Wang, Z.-B. Yang, H. Yu, F. Yan, S. Liu, et al., *Nature* **616**, 56 (2023).
- [8] S. J. Devitt, W. J. Munro, and K. Nemoto, *Rep. Prog. Phys.* **76**, 076001 (2013).
- [9] B. M. Terhal, *Rev. Mod. Phys.* **87**, 307 (2015).
- [10] L. Hu, Y. Ma, W. Cai, X. Mu, Y. Xu, W. Wang, Y. Wu, H. Wang, Y. Song, C.-L. Zou, et al., *Nat. Phys.* **15**, 503 (2019).
- [11] P. Campagne-Ibarcq, A. Eickbusch, S. Touzard, E. Zalgaller, N. E. Frattini, V. V. Sivak, P. Reinhold, S. Puri, S. Shankar, R. J. Schoelkopf, et al., *Nature* **584**, 368 (2020).
- [12] J. M. Gertler, B. Baker, J. Li, S. Shirol, J. Koch, and C. Wang, *Nature* **590**, 243 (2021).
- [13] S. Krinner, N. Lacroix, A. Remm, A. Di Paolo, E. Genois, C. Leroux, C. Hellings, S. Lazar, F. Swiadek, J. Herrmann, et al., *Nature* **605**, 669 (2022).
- [14] Y. Zhao, Y. Ye, H.-L. Huang, Y. Zhang, D. Wu, H. Guan, Q. Zhu, Z. Wei, T. He, S. Cao, et al., *Phys. Rev. Lett.* **129**, 030501 (2022).
- [15] R. Acharya, I. Aleiner, R. Allen, T. I. Andersen, M. Ansmann, F. Arute, K. Arya, A. Asfaw, J. Atalaya, B. Ryan, et al., *Nature* **614**, 676 (2023).
- [16] W. Yang, Z.-Y. Wang, and R.-B. Liu, *Front. Phys. China* **6**, 2 (2011).
- [17] L. Viola and S. Lloyd, *Phys. Rev. A* **58**, 2733 (1998).
- [18] L. Viola, E. Knill, and S. Lloyd, *Phys. Rev. Lett.* **82**, 2417 (1999).
- [19] L. Viola and E. Knill, *Phys. Rev. Lett.* **90**, 037901 (2003).
- [20] L. Viola and E. Knill, *Phys. Rev. Lett.* **94**, 060502 (2005).
- [21] K. Khodjasteh and D. A. Lidar, *Phys. Rev. Lett.* **95**, 180501 (2005).
- [22] W. Yang and R.-B. Liu, *Phys. Rev. Lett.* **101**, 180403 (2008).
- [23] H. Uys, M. J. Biercuk, and J. J. Bollinger, *Phys. Rev. Lett.* **103**, 040501 (2009).
- [24] J. Du, X. Rong, N. Zhao, Y. Wang, J. Yang, and R. Liu, *Nature* **461**, 1265 (2009).
- [25] K. Khodjasteh, D. A. Lidar, and L. Viola, *Phys. Rev. Lett.* **104**, 090501 (2010).
- [26] J. R. West, B. H. Fong, and D. A. Lidar, *Phys. Rev. Lett.* **104**, 130501 (2010).
- [27] G. De Lange, Z.-H. Wang, D. Riste, V. Dobrovitski, and R. Hanson, *Science* **330**, 60 (2010).
- [28] R. Rizzato, M. Schalk, S. Mohr, J. C. Hermann, J. P. Leibold, F. Bruckmaier, G. Salvitti, C. Qian, P. Ji, G. V. Astakhov, et al., *Nat. Commun.* **14**, 5089 (2023).
- [29] P. Zanardi, *Phys. Lett. A* **258**, 77 (1999).
- [30] L. Viola, E. Knill, and S. Lloyd, *Phys. Rev. Lett.* **85**, 3520 (2000).
- [31] L.-A. Wu, P. Zanardi, and D. Lidar, *Phys. Rev. Lett.* **95**, 130501 (2005).
- [32] J. Zhang, Z.-Y. Zhou, L.-A. Wu, and J. Q. You, *Phys. Rev. Applied* **11**, 044023 (2019).
- [33] J. Bylander, S. Gustavsson, F. Yan, F. Yoshihara, K. Harrabi, G. Fitch, D. G. Cory, Y. Nakamura, J.-S. Tsai, and W. D. Oliver, *Nat. Phys.* **7**, 565 (2011).
- [34] S. Gustavsson, F. Yan, J. Bylander, F. Yoshihara, Y. Nakamura, T. P. Orlando, and W. D. Oliver, *Phys. Rev. Lett.* **109**, 010502 (2012).
- [35] Q. Guo, S.-B. Zheng, J. Wang, C. Song, P. Zhang, K. Li, W. Liu, H. Deng, K. Huang, D. Zheng, et al., *Phys. Rev. Lett.* **121**, 130501 (2018).
- [36] B. Pokharel, N. Anand, B. Fortman, and D. A. Lidar, *Phys. Rev. Lett.* **121**, 220502 (2018).
- [37] Y. Sung, F. Beaudoin, L. M. Norris, F. Yan, D. K. Kim, J. Y. Qiu, U. von Lüpkke, J. L. Yoder, T. P. Orlando, S. Gustavsson, et al., *Nat. Commun.* **10**, 3715 (2019).
- [38] J. Qiu, Y. Zhou, C.-K. Hu, J. Yuan, L. Zhang, J. Chu, W. Huang, W. Liu, K. Luo, Z. Ni, et al., *Phys. Rev.*

- Applied **16**, 054047 (2021).
- [39] Supplementary Material for Protecting logical qubits with dynamical decoupling.
- [40] E. Kapit and V. Oganessian, ArXiv:2212.04588 (2022).
- [41] J. D. Teoh, P. Winkel, H. K. Babla, B. J. Chapman, J. Claes, S. J. de Graaf, J. W. Garmon, W. D. Kalfus, Y. Lu, A. Maiti, et al., Proc. Natl. Acad. Sci. U.S.A. **120**, e2221736120 (2023).
- [42] H. Levine, A. Haim, J. S. Hung, N. Alidoust, M. Kalaei, L. DeLorenzo, E. A. Wollack, P. A. Arriola, A. Khalajhedayati, Y. Vaknin, et al., ArXiv:2307.08737 (2023).
- [43] K. S. Chou, T. Shemma, H. McCarrick, T.-C. Chien, J. D. Teoh, P. Winkel, A. Anderson, J. Chen, J. Curtis, S. J. de Graaf, et al., ArXiv:2307.03169 (2023).
- [44] A. Kubica, A. Haim, Y. Vaknin, H. Levine, F. Brandão, and A. Retzker, Phys. Rev. X **13**, 041022 (2023).
- [45] F. Yan, P. Krantz, Y. Sung, M. Kjaergaard, D. L. Campbell, T. P. Orlando, S. Gustavsson, and W. D. Oliver, Phys. Rev. Applied **10**, 054062 (2018).
- [46] B. Foxen, C. Neill, A. Dunsworth, P. Roushan, B. Chiaro, A. Megrant, J. Kelly, Z. Chen, K. Satzinger, R. Barends, et al., Phys. Rev. Lett. **125**, 120504 (2020).
- [47] T. Roy, S. Kundu, M. Chand, V. M., A. Ranadive, N. Nehra, M. Patankar, J. Aumentado, A. Clerk, and R. Vijay, Appl. Phys. Lett. **107** (2015).
- [48] L. H. Pedersen, N. M. Møller, and K. Mølmer, Phys. Lett. A **367**, 47 (2007).
- [49] E. Magesan, R. Blume-Kohout, and J. Emerson, Phys. Rev. A **84**, 012309 (2011).
- [50] C. H. Bennett and S. J. Wiesner, Phys. Rev. Lett. **69**, 2881 (1992).
- [51] F. Zhang, J. Xing, X. Hu, X. Pan, and G. Long, AAPPS Bulletin **33**, 2 (2023).